Experimental Neurology 322 (2019) 113064

Contents lists available at ScienceDirect

Experimental Neurology

journal homepage: www.elsevier.com/locate/yexnr

Research paper

β_2-adrenergic receptor-mediated mitochondrial biogenesis improves skeletal muscle recovery following spinal cord injury

Natalie E. Scholpa[a], Epiphani C. Simmons[a,b], Douglas G. Tilley[c], Rick G. Schnellmann[a,b,d,e,f,*]

[a] Department of Pharmacology and Toxicology, College of Pharmacy, University of Arizona, Tucson, AZ, United States of America
[b] Department of Neurosciences, College of Medicine, University of Arizona, Tucson, AZ, United States of America
[c] Center for Translational Medicine, Lewis Katz School of Medicine, Temple University, Philadelphia, PA, United States of America
[d] Southern Arizona VA Health Care System, Tucson, AZ, United States of America
[e] Southwest Environmental Health Science Center, University of Arizona, Tucson, AZ, United States of America
[f] Center for Innovation in Brain Science, University of Arizona, Tucson, AZ, United States of America

ARTICLE INFO

Keywords:
Spinal cord injury
Mitochondrial biogenesis
Formoterol
β_2-adrenergic receptor
Skeletal muscle
Recovery

ABSTRACT

In addition to local spinal cord dysfunction, spinal cord injury (SCI) can result in decreased skeletal muscle mitochondrial activity and muscle atrophy. Treatment with the FDA-approved β_2-adrenergic receptor (ADRB2) agonist formoterol has been shown to induce mitochondrial biogenesis (MB) in both the spinal cord and skeletal muscle and, therefore, has the potential to address comprehensive mitochondrial and organ dysfunction following SCI. Female C57BL/6 mice were subjected to moderate contusion SCI (80 Kdyn) followed by daily administration of vehicle or formoterol beginning 8 h after injury, a clinically relevant time-point characterized by a 50% decrease in mtDNA content in the injury site. As measured by the Basso Mouse Scale, formoterol treatment improved locomotor recovery in SCI mice compared to vehicle treatment by 7 DPI, with continued recovery observed through 21 DPI (3.5 v. 2). SCI resulted in 15% body weight loss in all mice by 3 DPI. Mice treated with formoterol returned to pre-surgery weight by 13 DPI, while no weight gain occurred in vehicle-treated SCI mice. Remarkably, formoterol-treated mice exhibited a 30% increase in skeletal muscle mass compared to those treated with vehicle 21 DPI (0.93 v. 0.72% BW), corresponding with increased MB and decreased skeletal muscle atrophy. These effects were not observed in ADRB2 knockout mice subjected to SCI, indicating that formoterol is acting via the ADRB2 receptor. Furthermore, knockout mice exhibited decreased basal spinal cord and skeletal muscle PGC-1α expression, suggesting that ADRB2 may play a role in mitochondrial homeostasis under physiological conditions. These data provide evidence for systemic ADRB2-mediated MB as a therapeutic avenue for the treatment of SCI.

1. Introduction

There is a prevalence of approximately 290,000 persons and over 17,500 annual incidences of spinal cord injury (SCI) in the United States National Spinal Cord Injury Statistical Center, 2019. In general, life expectancy post-SCI is significantly below that of non-sufferers, with remaining years being inversely correlated with severity of neurological impairments National Spinal Cord Injury Statistical Center, 2019. While the most common causes of death post-SCI are pneumonia and septicemia, mortality rates for metabolic and musculoskeletal disorders are on the rise National Spinal Cord Injury Statistical Center, 2019.

Depending on the location and severity of the injury, consequences of SCI can range from loss of function to complete paralysis below the injury site, which can lead to skeletal muscle atrophy, with muscle area decreasing as much as 50% compared to that of healthy individuals (Castro et al., 1999). Regulation of muscle mass involves the cross-talk of multiple signaling pathways to coordinate protein synthesis and degradation (Bonaldo and Sandri, 2013). Induction of muscle atrophy

Abbreviations: ADRB2, β_2-adrenergic receptor; ATP Syn β, ATP synthase β; BMS, Basso Mouse Scale; DPI, days post-injury; EC, eriochrome cyanine; ETC, electron transport chain; FoxO, forkhead box protein O; IGC-1, insulin-like growth factor 1; KO, knockout; MB, mitochondrial biogenesis; mtDNA, mitochondrial DNA; MuRF-1, muscle RING-finger protein-1; PGC-1α, peroxisomal proliferator-activated γ coactivator 1α; SCI, spinal cord injury; TEM, transmission electron microscopy; TFAM, mitochondrial transcription factor A; WT, wild-type

* Corresponding author at: Department of Pharmacology and Toxicology, University of Arizona, Tucson, AZ 85721, United States of America.
E-mail addresses: scholpa@pharmacy.arizona.edu (N.E. Scholpa), esimmons@pharmacy.arizona.edu (E.C. Simmons), douglas.tilley@temple.edu (D.G. Tilley), schnell@pharmacy.arizona.edu (R.G. Schnellmann).

https://doi.org/10.1016/j.expneurol.2019.113064
Received 25 July 2019; Received in revised form 28 August 2019; Accepted 12 September 2019
Available online 13 September 2019
0014-4886/ Published by Elsevier Inc.

can occur through activation of myostatin, which is activated in muscle paralyzed by SCI (De Gasperi et al., 2016), and the forkhead box protein O (FoxO) family of transcription factors, which stimulate the transcription of atrophy-related genes, such as muscle RING-finger protein-1 (MuRF-1) (Bodine et al., 2001; Bonaldo and Sandri, 2013; Sandri et al., 2004). In contrast, hypertrophy is regulated by the insulin-like growth factor 1 (IGF-1)/Akt pathway, which stimulates protein synthesis (Bonaldo and Sandri, 2013). Activation of Akt can also attenuate atrophy via deactivating phosphorylation of FoxO transcription factors, sequestering them in the cytosol and inhibiting their transcriptional function (Brunet et al., 1999).

Loss of metabolically active muscle after SCI causes decreased basal metabolic activity, substantially decreasing energy expenditure and altering energy balance, ultimately contributing to altered body composition, increased fat mass and obesity (Gorgey et al., 2014; Monroe et al., 1998). Although the specific relationship is uncertain, body composition changes and decreased physical activity are considered fundamental to metabolic deterioration and the development of metabolic syndrome post-SCI, increasing the risk of type II diabetes and cardiovascular disease (Gorgey et al., 2014).

While spinal cord mitochondrial dysfunction is a widely accepted hallmark of SCI (Scholpa and Schnellmann, 2017), less is known regarding the disruption of skeletal muscle mitochondria post-SCI and its role in the onset of metabolism-related comorbidities. Paralysis post-SCI results in disuse atrophy, leading to a rapid loss of skeletal muscle function and metabolic activity (Gorgey et al., 2019). Interestingly, mitochondrial dysfunction has been shown to occur prior to muscle atrophy after SCI-induced paralysis (Gorgey et al., 2019). Studies have shown decreased mitochondrial size, protein expression and function in the skeletal muscle of SCI victims (Martin et al., 1992; McCully et al., 2011; Scelsi et al., 1982), similar to that observed with metabolic diseases such as obesity and type II diabetes (Kelley et al., 2002). It is important to note that the relationship between type II diabetes/obesity and skeletal muscle mitochondrial health remains uncertain. There is conflicting evidence on whether mitochondrial alterations are a cause or a consequence of insulin resistance in these metabolic disorders (Montgomery and Turner, 2015). Regardless, because of their role in energy metabolism, restoration of mitochondrial health may have the potential to decrease the severity of skeletal muscle metabolic dysfunction, and therefore disease onset or progression (O'Brien and Gorgey, 2016; Toledo and Goodpaster, 2013).

β_2-adenergic receptor (ADRB2) agonists such as the FDA-approved drug formoterol are known to increase skeletal muscle mass and activate muscle hypertrophy (Joassard et al., 2013; Sato et al., 2011). ADRB2 agonism has also been shown to prevent/attenuate muscle weakness and atrophy in animal models of muscular dystrophy, denervation and myotoxic injury (Beitzel et al., 2004; Harcourt et al., 2007; Zeman et al., 1987). Similarly, we reported that treatment with formoterol increased hypertrophy and prevented atrophy in the gastrocnemius in a dexamethasone-induced skeletal muscle atrophy mouse model (Jesinkey et al., 2014b).

Systemic formoterol administration increases the expression of peroxisomal proliferator-activated γ coactivator 1α (PGC-1α), a key transcriptional regulator of mitochondrial biogenesis (MB) (Scholpa et al., 2019) in multiple organ systems in mice, including the spinal cord (Scholpa et al., 2019) and skeletal muscle (Jesinkey et al., 2014b). As such, formoterol treatment has the potential to comprehensively address broad mitochondrial dysfunction. We previously showed that formoterol treatment beginning 1 h after SCI improves body weight, locomotor capability and spinal cord mitochondrial homeostasis (Scholpa et al., 2019). The effect of formoterol treatment on skeletal muscle post-SCI, however, remains undiscerned.

Multiple isoforms of PGC-1α exist, with PGC-1α1 being canonically responsible for the promotion of MB and mitochondrial gene expression (Jesinkey et al., 2014b; Martinez-Redondo et al., 2016). Interestingly, this isoform has also been shown to attenuate muscle atrophy via negative regulation of MuRF-1 (Jesinkey et al., 2014b; Qin et al., 2010). The isoform PGC-1α4, on the other hand is involved in the induction of IGF-1 and skeletal muscle hypertrophy, having no regulatory effects on mitochondrial targets of PGC-1α (Ruas et al., 2012). Given our previously published data indicating formoterol-induced PGC-1α expression in both skeletal muscle and the post-injured spinal cord, and the detrimental effects of dysregulated body composition and muscle metabolism after injury, we sought to determine the role of skeletal muscle atrophy and mitochondrial homeostasis on formoterol-induced recovery post-SCI in mice.

2. Materials and methods

2.1. Animals and SCI model

Female wild-type C57Bl/6 mice between 8 and 9 weeks of age were obtained from The Jackson Laboratories (Bar Harbor, ME), housed in groups of 3–5, and allowed to habituate for 7 days prior to use. Female ADRB2 knockout (KO) mice backcrossed onto a C57Bl/6 background were kindly provided by Dr. Douglas Tilley from Temple University (Grisanti et al., 2018).

To determine the mitochondrially biogenic effect of formoterol in the spinal cord under physiological conditions, naïve mice were treated with 0.1 mg/kg formoterol i.p. once daily for 48 h, followed by euthanasia via anesthesia overdose and isolation of the T9–13 region of the spinal cord and the gastrocnemius muscles.

For SCI studies, mice were randomized into sham and SCI groups. Animals were anesthetized with 10 mg/kg ketamine and 6 mg/kg xylazine via i.p injection and continuously monitored for spontaneous breathing. Mice underwent a complete single-level laminectomy at the 11th thoracic vertebrae (T11). The vertebral column was clamped and stabilized at the upper thoracic and lumbar levels, and a controlled contusion with a force of 80 kilodynes (Kdyn) and dwell time of 0 s was administered using the Infinite Horizon IH-0400 impactor (Lexington, KY) with the dura intact as previously described (Scholpa et al., 2019). Sham mice received laminectomy only. Manual bladder expression was performed twice daily until functional recovery. Injured mice were further divided into formoterol- or vehicle-treated groups. Animals were weighed daily and groups were euthanized 21d post-SCI via anesthesia overdose. Spinal cords were removed and gastrocnemius muscles were isolated and weighed. Tissues were flash frozen for analysis. All studies were approved by the Institutional Animal Care and Use Committee of the University of Arizona in accordance with the guidelines set forth by the National Institutes of Health *Guide for the Care and Use of Laboratory Animals*.

2.2. Drug treatment

Formoterol fumarate dehydrate was obtained from Sigma-Aldrich (St. Louis, MO) and dissolved in saline/1% DMSO to 0.01, 0.03 or 0.1 mg/mL. Mice were treated intraperitoneally (i.p) daily with either 0.1, 0.3, 1.0 mg/kg formoterol or vehicle control beginning 8 h after injury.

2.3. Transmission electron microscopy

Approximately 4 mm^2 samples of thoracic spinal cord and gastrocnemius were fixed overnight in 2.5% glutaraldehyde in 0.1 M PIPES buffer (pH 7.4) then transferred to PBS at which point they were delivered to the University of Arizona Microscopy Alliance, where they were placed in 0.1 M PIPES buffer (pH 7.4) overnight at 4 °C. Samples were then transferred to 0.1 M PIPES/Glycine buffer for 30 min at room temperature, then washed in deionized water (diH_2O) twice for 5 min each, placed in 1% osmium tetroxide for 1 h, washed twice in diH_2O for 10 min, then stained with 2% aqueous uranyl acetate for 1 h and washed again in diH_2O for 10 min. Samples were then dehydrated with

increasing ethanol dilutions (5 min, 50, 70, 90, 100%) and acetone (2 × 5min), infiltrated with 1:1 acetonitrile/Spurr's resin overnight, then 100% Spurr's resin for 24 h and flat-embedded overnight at 60 °C. Sections (80 nm) were cut on an RMC PTXL ultramicrotome, placed onto uncoated 150-mesh coper grids and counterstained with 2% lead acetate for 2 min. Spinal cord and skeletal muscle sections were viewed with an FEI Tecnai Spirit Transmission Electron Microscope (Hillsboro, OR) operated at 100 kV and TIFF images (8 bit) captured via an AMT XR41 CCD digital camera (Woburn, MA) at a magnification of 8200X, creating an 11.95 × 11.95 μm field, or 11,500× creating an 8.96 × 8.96 μm field, respectively. For the spinal cord, images of the white matter, particularly myelinated axons were captured. In all cases, 4–5 images were analyzed per sample and the average mitochondrial number and area per field calculated.

2.4. Locomotor capability assessment

Locomotor capability was assessed using the ten-point (0–9) Basso Mouse Scale (BMS) (Basso et al., 2006) by an observer blinded to experimental groups. Each mouse was observed for 3 min, with bladder expression taking place prior to assessment. Animals were observed 24 h after surgery and every other day thereafter until euthanasia. Sham animals maintained a BMS score of 9 throughout the experiment.

2.5. RNA expression

Total RNA was extracted from the spinal cord and skeletal muscle using TRIzol reagent (Invitrogen, Carlsbad, CA) based on the manufacturer's protocol. cDNA was synthesized using the iScript cDNA Synthesis Kit and qPCR performed using 500 ng of cDNA template and SsoAdvanced Universal SYBR Green Supermix (Bio-Rad, Hercules, CA). Fold changes were calculated using the ΔΔCt method. The primers used can be found in Table 1.

2.6. mtDNA content

DNA was isolated from the spinal cord and skeletal muscle using the Qiagen DNeasy Blood and Tissue Kit (Valencia, CA) and 5 ng used for qPCR quantification of relative mitochondrial DNA (mtDNA) content. ND1, a mitochondrial gene, was measured and normalized to the nuclear encoded gene β-actin.

2.7. Immunoblot

Protein was extracted from the spinal cord and skeletal muscle using RIPA buffer (50 mM Tris-HCl, 150 mM NaCl, 0.1% SDS, 0.5% sodium deoxycholate, 1% Triton X-100, pH 7.4) with protease inhibitor cocktail (1:100), 1 mM sodium fluoride and 1 mM sodium orthovanadate (Sigma-Aldrich, St. Louis, MO). Samples were agitated for 2 h at 4 °C and then centrifuged at 14,000 ×*g* for 15 min and the supernatant collected. Protein was quantified using a bicinchoninic acid assay, and 10–12 μg of protein was separated via electrophoresis using 4–15% SDS-PAGE gels, then transferred to nitrocellulose membranes (Bio-Rad, Hercules, CA). Membranes were blocked in 5% milk or BSA in TBST and incubated overnight with primary antibodies with constant agitation at 4 °C. Membranes were incubated with the appropriate horseradish peroxidase-conjugated secondary antibody and visualized using chemiluminescence (Thermo Scientific, Waltham, MA) on a GE ImageQuant LAS4000 (GE Life Sciences, Pittsburg, PA). Optical density was determined using Image Studio Lite software. Primary antibodies used were as follows: MuRF-1 (1:1000, ECM Biosciences, Versailles, KY), p-Akt (S473, 1:1000, Cell Signaling, Danvers, MA), t-Akt (1:1000, Cell Signaling), p-FoxO1 (S256, 1:1000, Cell Signaling, Danvers, MA), t-FoxO1 (1:1000, Abcam, Cambridge, UK), PGC-1α (1:1000, Abcam), TFAM (1:1000, Abcam), ATP Syn β (1:1000, Abcam), α-tubulin (1:1000, Abcam), GAPDH (1:1000, Abcam).

2.8. Histopathological analysis

Spinal cord tissues were processed as previously described (Scholpa et al., 2019). Briefly, mice were transcardially perfused with 0.1 M PBS followed by 4% paraformaldehyde (PFA). A 6 mm segment centered on the injury sight was frozen in OCT at −80 °C and cryosectioned into 10 μm coronal sections. Eriochrome cyanine (EC) staining for myelin was used to distinguish damaged and spared tissue (Patel et al., 2017; Scholpa et al., 2019). Analyses were performed in a blinded fashion, with respect to treatment group, using an Aperio AT2 Slide Scanner and ImageScope software (Leica, Buffalo Grove, IL). Lesion and percent spared tissue areas were quantified across 2 mm of spinal cord centered on the epicenter at 100 μm intervals using the Cavalieri method (Patel et al., 2017; Scholpa et al., 2019), totaling 21 sections per animal.

2.9. Statistical analysis

Tissue isolated from a single animal or a single animal's behavior represented $n = 1$. Number of mice used for each analysis can be found in the Figure Legends. For behavior and body weight, data were analyzed using Two-way ANOVA with repeated measures followed by Tukey's post-hoc test. Differences between two groups were analyzed using two-tailed student's *t*-test, while that of three groups was analyzed using One-way ANOVA followed by Tukey's post-hoc test. In all cases, GraphPad Prism software (La Jolla, CA) was used and a $p < 0.05$ was considered indicative of a statistically significant difference between mean values.

3. Results

3.1. Effect of formoterol on mitochondrial content in the naïve spinal cord and skeletal muscle

Naïve mice were treated with 0.1 mg/kg formoterol or vehicle i.p. daily for 48 h. Following treatment, the T9–13 portion of the thoracic spinal cord and the gastrocnemius muscles were extracted. Transmission electron microscopy (TEM) was used to assess mitochondrial content (Fig. 1A). The spinal cords, specifically myelinated axons, and skeletal muscle of formoterol-treated mice displayed

Table 1
Primers.

Target	Sense	Antisense
ADRB2	5'-GTACCGTGCCACCCACAAGA-3'	5'-CCCGGGAATAGACAAAGACCATC-3'
β-Actin	5'-GGGATGTTTGCTCCAACCAA-3'	5'-GCGCTTTTGACTCAGGATTTAA-3'
IGF-1	5'-TGCTCTTCAGTTCGTGTG-3'	5'-ACATCTCCAGTCTCCTCAG-3'
Myostatin	5'-AGTGGATCTAAATGAGGGCAGT-3'	5'-GTTTCCAGGCGCAGCTTA-3'
ND1	5'-TGAATCCGAGCATCCTACC-3'	5'-ATTCCTGCTAGGAAAATTGG-3'
PGC-1α	5'-AGGAAATCCGAGCGGAGCTGA-3'	5'-GCAAGAAGGCGACACATCGAA-3'
PGC-1α1	5'-GGACATGTGCAGCCAAGACTCT-3'	5'-CACTTCAATCCACCCAGAAAGCT-3'
PGC-1α4	5'-TCACACCAAACCCACAGAAA-3'	5'-CTGGAAGATATGGCACAT-3'

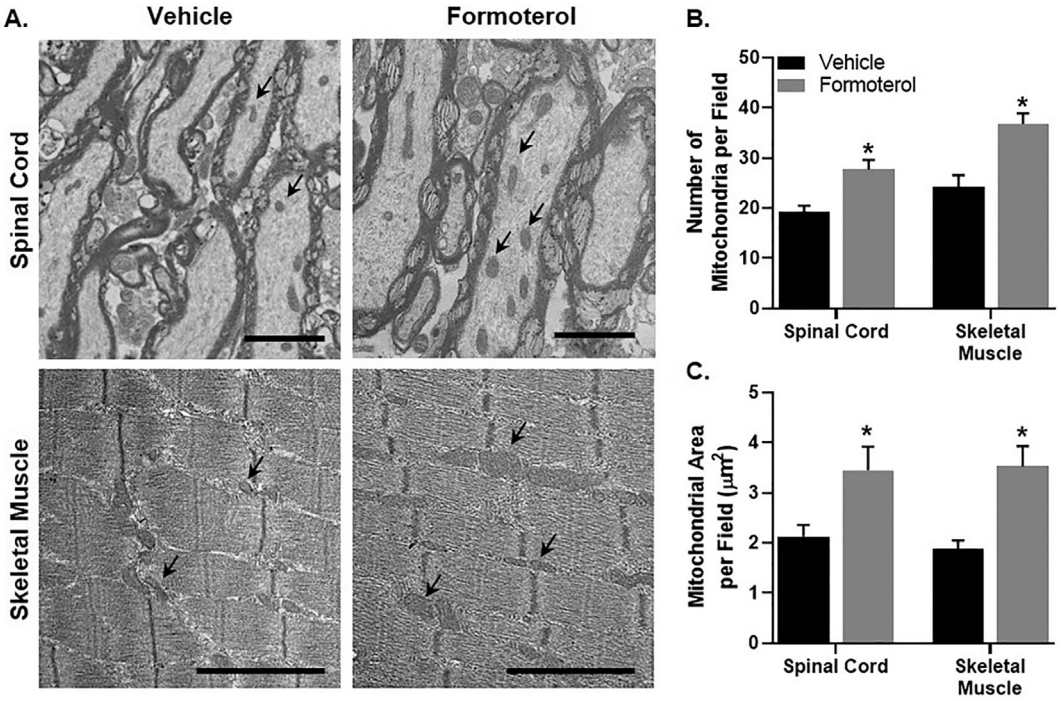

Fig. 1. Effect of formoterol on mitochondrial content in naïve mice. Mice were treated with vehicle or formoterol (0.1 mg/kg, i.p) daily for 48 h. The spinal cords and gastrocnemius muscle were extracted and imaged using transmission electron microscopy (*A*) to obtain the number of mitochondria (*B*) and mitochondrial area (*C*) per 11.95 × 11.95 μm or 8.96 × 8.96 μm field, respectively. Data are representative of 5 mice per group and are expressed as mean ± SEM. Scale bar = 2 μm (**p < 0.05 by Student's t-test*).

increases in both mitochondrial number (Fig. 1B) and area (Fig. 1C) per field. These data corroborate previously reported studies with formoterol (Jesinkey et al., 2014a; Scholpa et al., 2019; Wills et al., 2012).

3.2. Dose-response effect of formoterol on locomotor capability post-SCI

Mice were subjected to a force-controlled impactor-induced contusion model of SCI using a force of 80 Kdyn. Using this model, 8 h after injury mtDNA content was decreased nearly 50% in the injury site (Fig. 2A), indicating substantial mitochondrial dysfunction, similar to that observed previously with this model (Scholpa et al., 2019). Injured mice were treated daily with vehicle, 0.1, 0.3 or 1.0 mg/kg formoterol i.p beginning 8 h after injury and continuing until euthanasia. Locomotor capability was assessed using the Basso Mouse Scale (BMS), a 10-point scale ranging from complete paralysis (0) to normal hindlimb function (9) (Basso et al., 2006), beginning 24 h after injury and continuing every alternate day for 21 DPI. As expected, injured mice displayed complete hindlimb paralysis 24 h post-SCI and sham controls maintained normal function for the duration of the study (Scholpa et al., 2019). While increased BMS score compared to SCI + vehicle was observed with all doses of formoterol, injured mice treated with 0.3 mg/kg displayed improvement at 7 DPI, while improvement was not observed in those treated with 0.1 or 1.0 mg/kg until 11 DPI (Fig. 2B). The 0.3 mg/kg group reached a final BMS score of 3.5 (consistent dorsal/occasion plantar stepping) by 21 DPI, compared to a score of 2 (ankle movement) in vehicle-treated injured mice and 3.1 in injured mice treated with either 0.1 or 1.0 mg/kg formoterol. Based on these data, 0.3 mg/kg formoterol was used for the remainder of the studies.

3.3. Effect of formoterol on mitochondrial homeostasis and lesion volume post-SCI

Consistent with previously reported data (Scholpa et al., 2019), the expression of MB-related proteins PGC-1α and ATP synthase β (ATP Synβ), a subunit of ATP synthase of the electron transport chain (ETC) were decreased 3 DPI in the injury site of vehicle-treated injured mice. These decreases were attenuated by daily treatment with 0.3 mg/kg formoterol beginning 8 h after injury, with ATP Synβ in formoterol-treated injured mice being comparable to sham levels (Fig. 2C).

Lesion volume was assessed using Eriochrome cyanine staining for myelin (Fig. 2D) 21 DPI. Analysis of 2 mm of spinal cord centered on the injury epicenter revealed decreased lesion volume (Fig. 2E) and increased percent spared tissue (Fig. 2F) in injured mice treated with 0.3 mg/kg formoterol compared to that of vehicle-treated mice. Importantly, total volume analyzed was not different between treatment groups (Fig. 2G).

3.4. Effect of formoterol on body weight and skeletal muscle weight post-SCI

Animals were weighed prior to surgery (day 0) and on the same day as BMS assessment throughout the experiment. While all mice subjected to SCI exhibited 15% weight loss by 3 DPI, injured mice treated with 0.3 mg/kg formoterol displayed increased body weight compared to vehicle-treated injured mice by day 5. Furthermore, formoterol-treated mice returned to pre-surgery weight by 13 DPI, while no weight gain was observed in vehicle-treated SCI mice (Fig. 3A).

Left and right gastrocnemius muscles were isolated and weighed 21 DPI. To account for whole body differences between mice, combined gastrocnemius weight was normalized to obtain muscle mass as a percent of total body weight. Sham controls exhibited a gastrocnemius muscle mass of approximately 1% total body weight, similar to that reported previously in female mice (Graham et al., 2016). Muscle mass decreased nearly 30% to 0.72% body weight post-SCI in vehicle-treated mice. In injured mice treated with formoterol, however, the gastrocnemius muscles comprised 0.93% total body weight, comparable to that of sham mice (Fig. 3B).

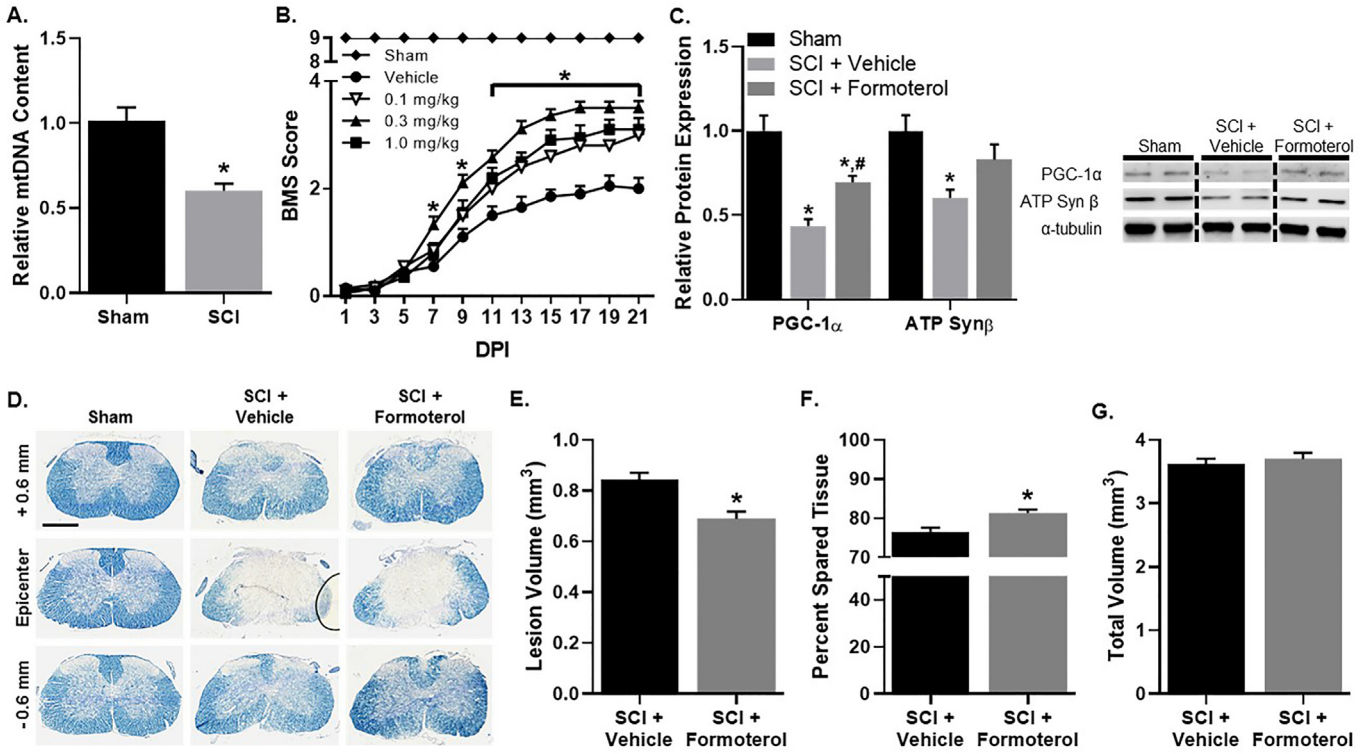

Fig. 2. Effect of formoterol following SCI in mice. Mice were subjected to moderate SCI using an 80 Kdyn force-controlled impactor-induced contusion model followed by daily administration of vehicle or formoterol (0.1–1.0 mg/kg, i.p) beginning 8 h post-injury, at which point mtDNA content is decreased nearly 50% (*A*) and continuing for up to 21 DPI. (*B*) Locomotor function was assessed using the Basso-Mouse scale beginning 24 h after injury and continuing every alternate data. Data are representative of 10 sham and 14 injured mice per group and are expressed as mean ± SEM. Bracket indicates time-points at which all doses are significantly different from SCI + Vehicle (*$p < 0.05$ by Two-Way ANOVA with repeated measures followed by Tukey's post-hoc test*). (*C*) A subset of mice was euthanized 3 DPI and the injury site extracted and analyzed for mitochondrial protein expression. Data are representative of 5 sham and 6 injured mice per group and are expressed as mean ± SEM (*$p < 0.05$ compared to Sham, #$p < 0.05$ compared to SCI + Vehicle by One-Way ANOVA followed by Tukey's post-hoc test*). (*D*) A subset of mice was euthanized 21 DPI and the spinal cords were extracted, stained with Eriochrome cyanine and analyzed for lesion volume (*E*), percent spared tissue (*F*) and total volume (*G*) across 2 mm of cord. Data are representative of 6 vehicle-treated and 5 formoterol-treated injured mice and are expressed as mean ± SEM. Scale bar = 0.5 mm (*$p < 0.05$ compared to SCI + Vehicle by Student's t-test*).

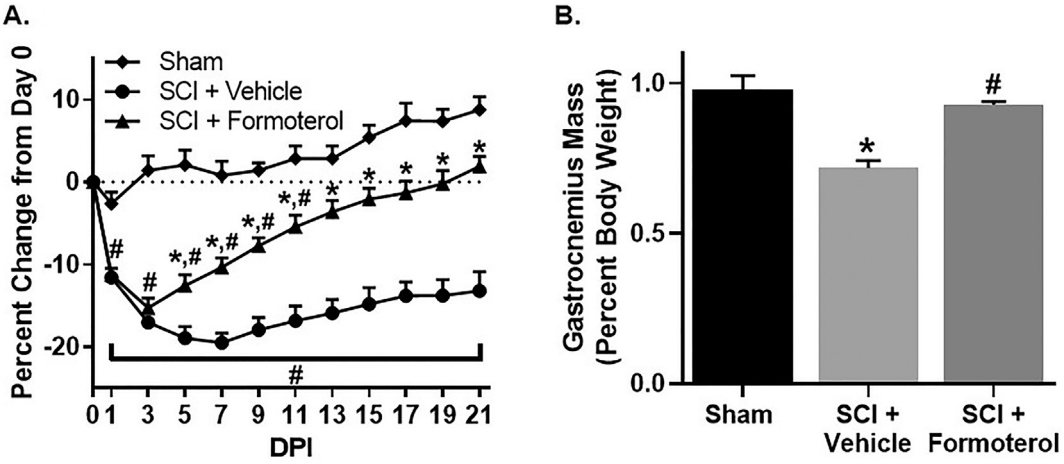

Fig. 3. Effect of formoterol on body weight and skeletal muscle mass following SCI in mice. Mice were subjected to moderate SCI using an 80 Kdyn force-controlled impactor-induced contusion model followed by daily administration of vehicle or formoterol (0.3 mg/kg, i.p) beginning 8 h post-injury and continuing for 21 DPI. (*A*) Body weight was assessed prior to injury (Day 0) and every day locomotor function was assessed. Data are representative of 10 sham and 14 injured mice per group and are expressed as mean ± SEM of the percent change from pre-surgery weight (*$p < 0.05$ compared to SCI + Vehicle, #$p < 0.05$ compared to Day 0 by Two-Way ANOVA with repeated measures followed by Tukey's post-hoc test*). (*B*) Left and right gastrocnemius muscles were extracted and weighed 21 DPI. Data are representative of 5 sham and 8 injured mice per group and are expressed as mean ± SEM of combined muscle mass as a percent of body weight (*$p < 0.05$ compared to Sham, #$p < 0.05$ compared to SCI + Vehicle by One-Way ANOVA followed by Tukey's post-hoc test*).

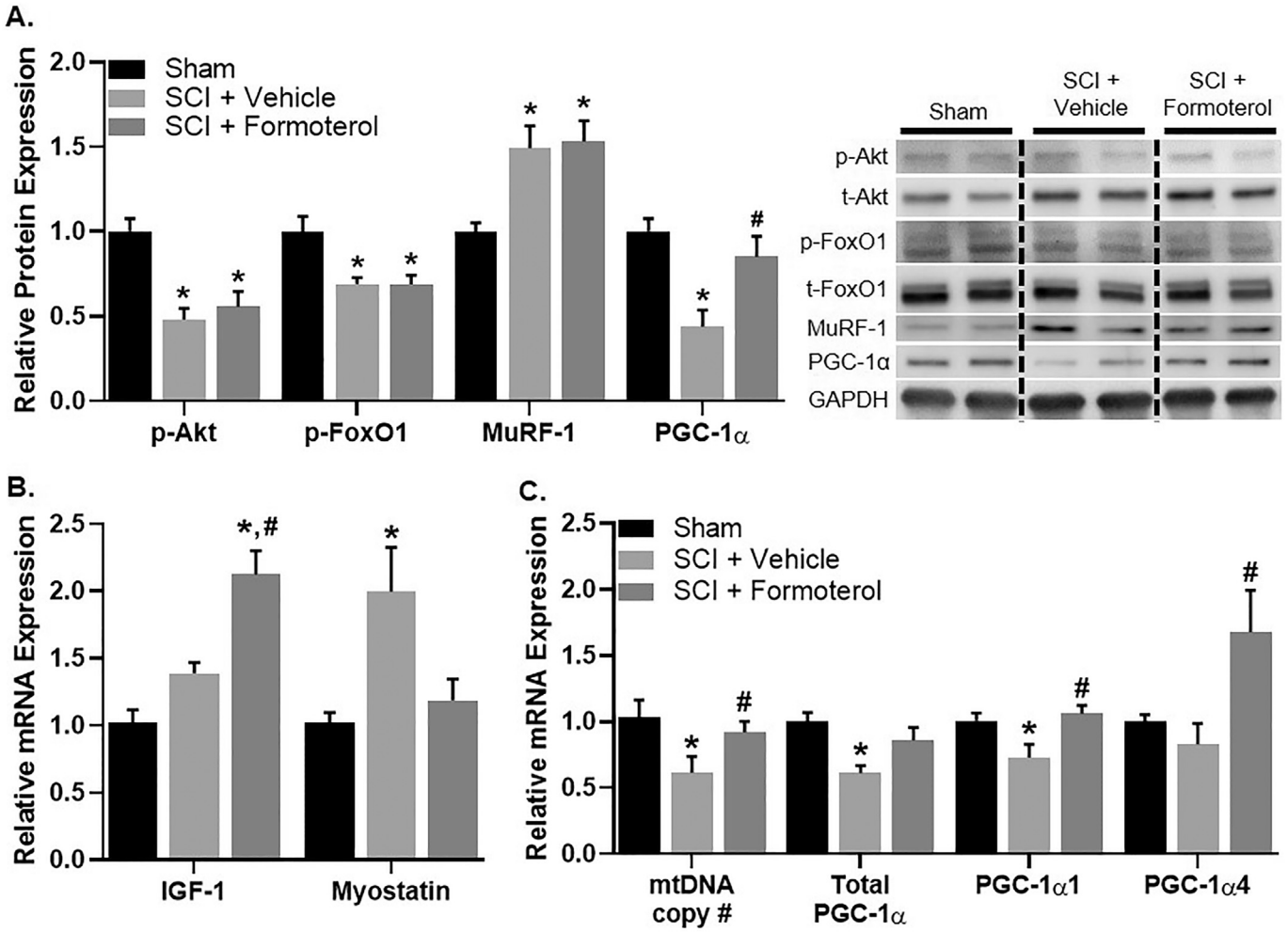

Fig. 4. Effect of formoterol on skeletal muscle atrophy/hypertrophy 3 DPI in mice. Mice were subjected to moderate SCI using an 80 Kdyn force-controlled impactor-induced contusion model followed by daily administration of vehicle of formoterol (0.3 mg/kg, i.p) beginning 8 h post-injury. A subset of mice was euthanized 3 DPI and the gastrocnemius muscles extracted and analyzed for protein (*A*) and mRNA (*B*) expression of atrophy and hypertrophy markers, as well as mtDNA and PGC-1α isoforms (*C*). Data are representative of 5 sham and 6 injured mice per group and are expressed as mean ± SEM (*$p < 0.05$ compared to Sham, #$p < 0.05$ compared to SCI + Vehicle by One-Way ANOVA followed by Tukey's post-hoc test).

3.5. Effect of formoterol on skeletal muscle atrophy and mitochondrial homeostasis post-SCI

By 3 DPI, p-Akt and p-FoxO1 were decreased in the skeletal muscle of injured mice regardless of treatment. Protein expression of MuRF-1, which is involved in protein degradation during skeletal muscle atrophy, was increased 3 DPI in injured mice (Fig. 4A). While no effect was observed on gene expression of the hypertrophy marker IGF-1, myostatin mRNA expression increased nearly 2-fold in vehicle-treated injured mice 3 DPI. Formoterol-treated injured mice exhibited increased gastrocnemius IGF-1 mRNA expression compared to both sham and vehicle-treated injured mice at 3 DPI. Additionally, myostatin was comparable to sham levels in the skeletal muscle of formoterol-treated injured mice (Fig. 4B).

Vehicle-treated injured mice exhibited decreased PGC-1α protein expression in the gastrocnemius 3 DPI, indicating impaired mitochondrial biogenesis; this decrease did not occur in the skeletal muscle of formoterol-treated injured mice (Fig. 4A). A similar effect was observed with gastrocnemius mtDNA content at this time point (Fig. 4C).

Similar to that observed with protein, total PGC-1α mRNA expression was decreased in vehicle-treated SCI mice, but not formoterol-treated SCI mice (Fig. 4C). By 3 DPI, expression of the PGC-1α1 isoform paralleled that of total PGC-1α, being decreased in the skeletal muscle of vehicle-treated injured mice and increased to sham levels in that of formoterol-treated injured mice. Interestingly, there was no effect on expression of the PGC-1α4 isoform in injured mice treated with vehicle; however, formoterol-treated injured mice displayed a 1.5 fold increase in gastrocnemius mRNA expression of this isoform compared to SCI mice treated with vehicle (Fig. 4C).

By 21 DPI, p-Akt and p-FoxO1 remained decreased, and MuRF-1 remained elevated in the skeletal muscle of vehicle-treated injured mice. Formoterol-treated injured mice displayed increased p-Akt and p-FoxO1, as well as decreased MuRF-1 in the skeletal muscle compared to those treated with vehicle, with p-Akt and MuRF-1 being no different from sham controls (Fig. 5A). Similar to that observed 3 DPI, formoterol-treated SCI mice displayed increased IGF-1 mRNA expression compared to both sham and vehicle-treated injured mice 21 DPI. While myostatin remained increased in vehicle-treated SCI mice, that of injured mice treated with formoterol decreased to 40% of sham levels by this time point (Fig. 5B).

While no differences were observed in PGC-1α protein expression by 21 DPI (Fig. 5A), decreased mtDNA content persisted in the skeletal muscle of vehicle-treated injured mice; again, formoterol treatment restored mtDNA content to sham levels (Fig. 5C). Comparable to protein expression, no differences were observed in total PGC-1α mRNA expression or in either isoform investigated.

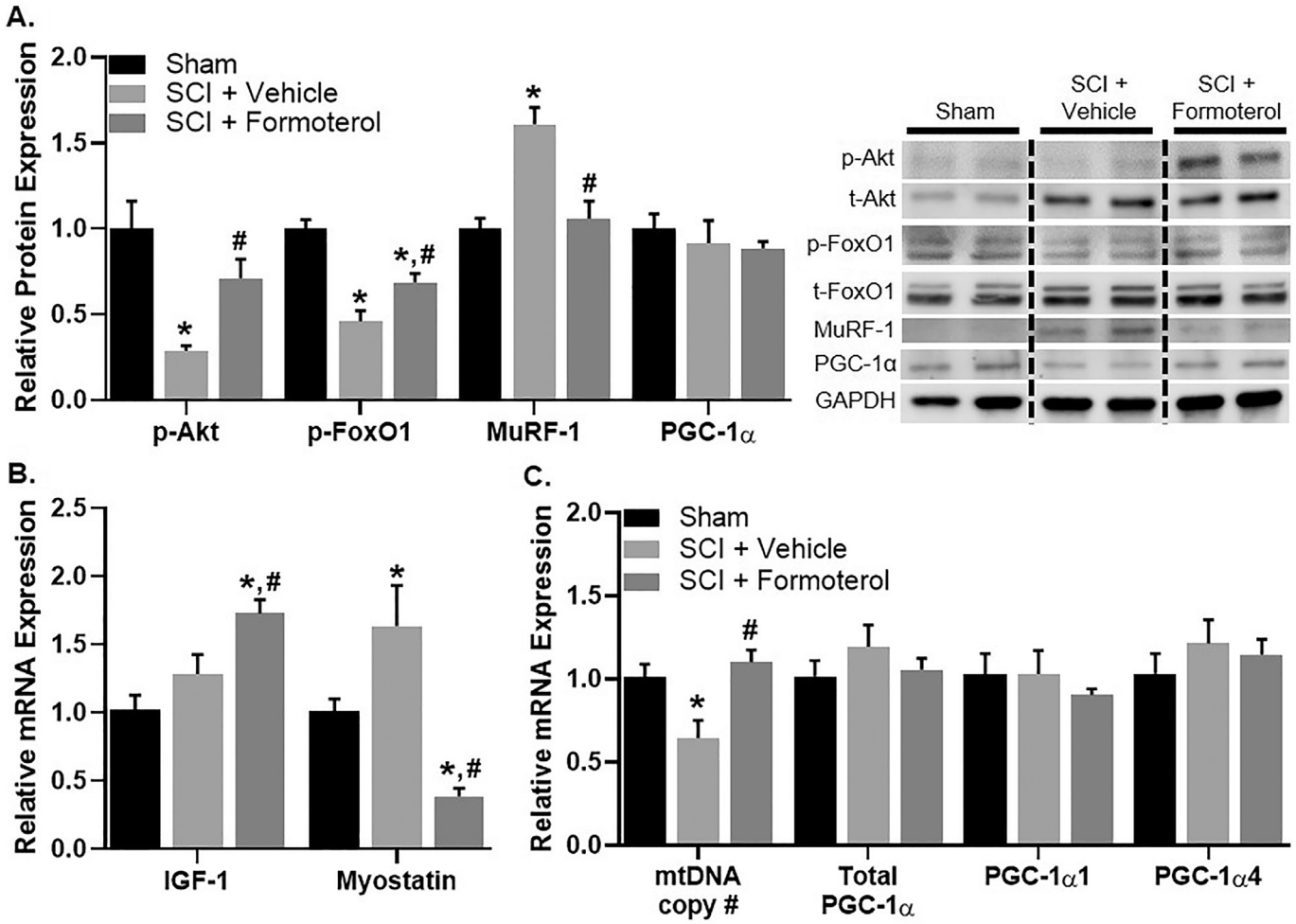

Fig. 5. Effect of formoterol on skeletal muscle atrophy/hypertrophy 21 DPI in mice. Mice were subjected to moderate SCI using an 80 Kdyn force-controlled impactor-induced contusion model followed by daily administration of vehicle of formoterol (0.3 mg/kg, i.p) beginning 8 h post-injury. A subset of mice was euthanized 21 DPI and the gastrocnemius muscles extracted and analyzed for protein (*A*) and mRNA (*B*) expression of atrophy and hypertrophy markers, as well as mtDNA and PGC-1α isoforms (*C*). Data are representative of 5 sham and 6 injured mice per group and are expressed as mean ± SEM (*$p < 0.05$ compared to Sham, #$p < 0.05$ compared to SCI + Vehicle by One-Way ANOVA followed by Tukey's post-hoc test).

3.6. Effect of ADRB2 loss under physiological conditions and post-SCI

Lack of ADRB2 was confirmed in the spinal cord and gastrocnemius (not shown) of naïve 9 week old female *ADRB2*$^{-/-}$ (KO) mice via PCR (Fig. 6A). Protein analysis revealed decreased expression of PGC-1α and mitochondrial transcription factor A (TFAM) in both the spinal cord (Fig. 6B) and gastrocnemius (Fig. 6C) of KO mice compared to wild-type (WT) mice, suggesting altered basal mitochondrial homeostasis.

WT and KO mice were subjected to SCI followed by daily formoterol administration that continued for 21 DPI. The purpose of this experiment was to determine if the observed effects of formoterol were reliant on ADRB2 agonism; therefore, treatment with 0.1 mg/kg formoterol (i.p) was initiated 1 h after injury to parallel previous studies (Scholpa et al., 2019). Similar to that reported previously, vehicle-treated injured WT mice exhibited a BMS score of approximately 2 by 21 DPI (Fig. 7A). Additionally, injured WT mice treated with formoterol displayed an increased BMS score compared to vehicle-treated SCI WT mice by 7 DPI, reaching 3.6 by 21 DPI. Comparable to WT, vehicle-treated injured KO mice also depicted a final BMS score of approximately 2 by 21 DPI (Fig. 7A). Unlike in WT mice, formoterol treatment had no effect on BMS score in injured KO mice.

All injured mice regardless of treatment or genotype exhibited a 15% loss in body weight by 3 DPI (Fig. 7B). The body weight of injured WT formoterol-treated mice increased compared to that of vehicle-treated SCI WT mice by 7 DPI, returning to pre-surgery weight by day 13. No difference was observed between formoterol- or vehicle-treated injured KO mice (Fig. 7B).

Gastrocnemius muscles of all mice were isolated and weighed 21 DPI and normalized to total body weight. Sham mice of both genotypes exhibited a muscle mass of approximately 1% body weight. After injury, muscle mass was decreased ~25% in both vehicle-treated WT and KO mice. Similar to that shown in Fig. 3B, the gastrocnemius mass of formoterol-treated injured WT mice was comparable to that of sham mice. Conversely, formoterol had no effect on muscle mass in injured KO mice, with formoterol- and vehicle-treated SCI KO mice exhibiting similar degrees of muscle loss (Fig. 7C).

4. Discussion

Mitochondrial dysfunction within the spinal cord is a well-established consequence of SCI and is the target of ongoing research into potential therapeutic strategies. Skeletal muscle mitochondrial dysfunction post-SCI, however, is less understood. Depending on the severity, SCI can result in varying degrees of mobility loss below the level of injury. Consequently, the resulting skeletal muscle atrophy increases the risk of development of metabolic diseases such as type II diabetes and obesity (O'Brien and Gorgey, 2016). Recently, such diseases have also been associated with mitochondrial dysfunction (Hojlund et al.,

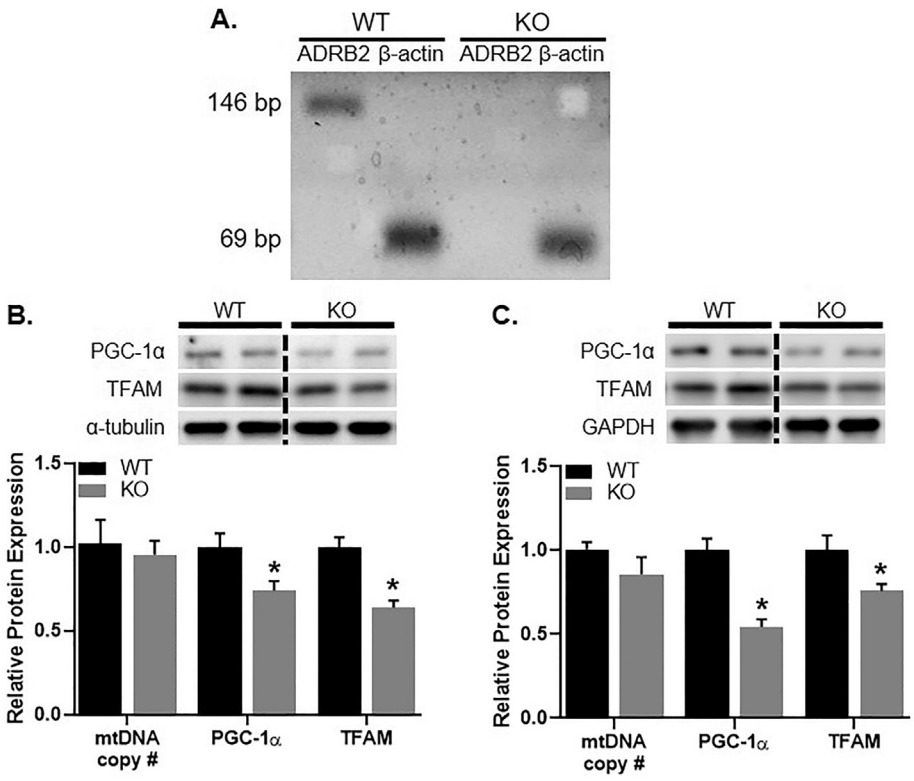

Fig. 6. Effect of lacking ADRB2 on basal mitochondrial homeostasis. (*A*) PCR was used to confirm the presence of ADRB2 in the spinal cord of wild-type (WT) mice, and the lack thereof in *ADRB2*$^{-/-}$ (KO) mice. The spinal cord (*B*) and gastrocnemius muscle (*C*) were extracted from naïve WT and KO mice and assessed for mitochondrial protein expression. Data are representative of 5 mice per group and are expressed as mean ± SEM (*$p < 0.05$ by Student's t-test*).

2008), indicating the significance of broad mitochondrial health post-SCI.

We assessed the therapeutic efficacy of systemic pharmacological induction of MB using the FDA-approved ADRB2 agonist formoterol post-SCI, with treatment initiation beginning 8 h after injury, when substantial mitochondrial dysfunction was present. Remarkably, all doses (0.1, 0.3, 1 mg/kg) of formoterol improved locomotor capability; however, the recovery was greater and occurred sooner post-injury with a dose of 0.3 mg/kg. Similar to what we reported previously (Scholpa et al., 2019), decreased MB-related protein expression, including PGC-1α, was observed in the injury site by 3 DPI and was attenuated with formoterol treatment, indicating that even with delayed initiation, formoterol treatment induces MB in the injured spinal cord. Additionally, this delayed formoterol initiation resulted in increased tissue sparing in the spinal cord 21 DPI, further advocating the therapeutic potential of this treatment strategy post-SCI.

Metabolic disorders including obesity are prevalent following SCI; however, within the first year after injury, a majority of victims experience significant weight loss (Landry et al., 2004; Powell et al., 2017). We observed decreased body weight as early as 1 DPI in all injured animals. Interestingly, this decrease persisted in vehicle-treated mice, indicating sustained disruption of body composition in these animals. Conversely, formoterol-treated mice exhibited increased body weight as early as 5 DPI and returned to pre-surgery weight by day 13, suggesting reestablishment of normal body composition. This is further supported by the restoration of gastrocnemius muscle mass in

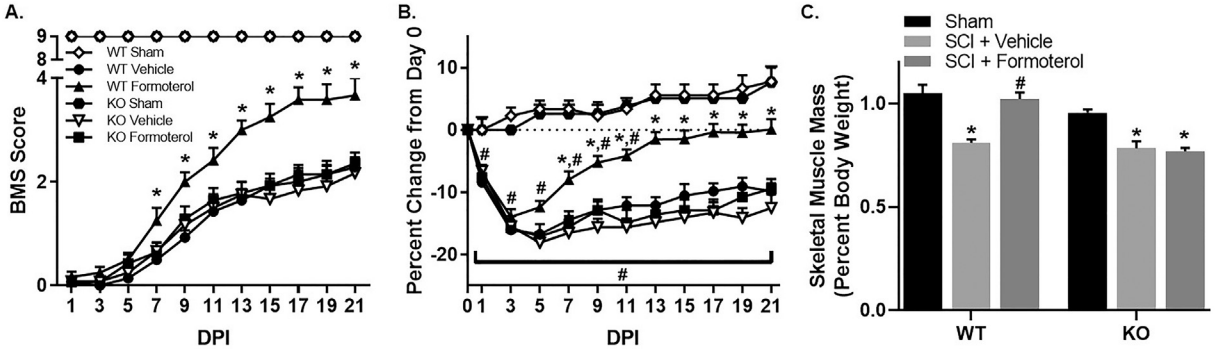

Fig. 7. Effect of lacking ADRB2 on formoterol-induced recovery following spinal cord injury in mice. Wild-type (WT) and *ADRB2*$^{-/-}$ (KO) mice were subjected to moderate SCI using an 80 Kdyn force-controlled impactor-induced contusion model followed by daily administration of vehicle or formoterol (0.1 mg/kg, i.p) beginning 1 h post-injury and continuing for 21 DPI. (*A*) Locomotor function was assessed using the Basso-Mouse scale beginning 24 h after injury and continuing every alternate data. Data are representative of 5 sham and 8 injured mice per group and are expressed as mean ± SEM. (*$p < 0.05$ compared to WT Vehicle by Two-Way ANOVA with repeated measures followed by Tukey's post-hoc test*). (*B*) Body weight was assessed prior to injury (Day 0) and every day locomotor function was assessed. Data are representative of 5 sham and 8 injured mice per group and are expressed as mean ± SEM of the percent change from pre-surgery weight (*$p < 0.05$ compared to WT Vehicle, #$p < 0.05$ compared to Day 0 by Two-Way ANOVA with repeated measures followed by Tukey's post-hoc test*). (*C*) Left and right gastrocnemius muscles were extracted and weighed 21 DPI. Data are representative of 5 sham and 8 injured mice per group and are expressed as mean ± SEM of combined muscle mass as a percent of body weight (*$p < 0.05$ compared to Sham, #$p < 0.05$ compared to SCI + Vehicle by One-Way ANOVA followed by Tukey's post-hoc test*).

formoterol-treated SCI mice by 21 DPI.

Regardless of the cause, muscle loss is accompanied by transcriptional changes (Sandri et al., 2006). Activated FoxO1 is increased in multiple models of muscle atrophy (Lecker et al., 2004; Sandri et al., 2004). FoxO1 can be phosphorylated by Akt, resulting in deactivation and prevention of the transcription of many atrophy-related genes, including MuRF-1. Formoterol has been shown to activate Akt in multiple systems, including a mouse model of skeletal muscle atrophy (Jesinkey et al., 2014c). Consistent with reports in humans, we observed increased MuRF-1 expression in the skeletal muscle by 3 DPI (Urso et al., 2007). We also observed decreased p-Akt and p-FoxO1 protein expression in the gastrocnemius 3 DPI regardless of treatment; however, formoterol-treated mice exhibited protein expression levels largely comparable to sham controls by 21 DPI. These data indicate that formoterol administration post-SCI activated Akt in the skeletal muscle, thereby increasing FoxO1 phosphorylation, leading to its deactivation and subsequent decreased transcription of atrophy genes, including MuRF-1. Therefore, while skeletal muscle atrophy persisted in vehicle-treated mice, muscle health was improved in those treated with formoterol, likely contributing to restoration of body composition, muscle mass and functional recovery.

Corresponding with our observations 3 DPI, skeletal muscle PGC-1α expression has been shown to decrease substantially in various models of muscle wasting, including following SCI (Gorgey et al., 2019; Jesinkey et al., 2014b; Sandri et al., 2006). Formoterol-treatment returned skeletal muscle PGC-1α expression to that of sham levels as early as 3 DPI. This effect was also observed with mtDNA copy number. In addition to total PGC-1α, we also assessed the expression of the PGC-1α1 isoform, which is associated with MB (Martinez-Redondo et al., 2016). Consistent with total PGC-1α and mtDNA content, PGC-1α1 was decreased in the skeletal muscle following injury and returned to sham levels with formoterol-treatment by 3 DPI. Taken together, these data indicate early formoterol-induced MB in the skeletal muscle, similar to that which occurred in the spinal cord.

Along with its principal role in mitochondrial function and MB, PGC-1α is also involved in muscle hypertrophy (Martinez-Redondo et al., 2016). Expression of PGC-1α4, which is known to activate IGF-1 and repress myostatin (Ruas et al., 2012), was increased in the skeletal muscle of formoterol-treated mice 3 DPI, corresponding to increased IGF-1 and decreased myostatin mRNA expression. While PGC-1α4 is generally associated with muscle health, PGC-1α1, in addition to its established mitochondrial effects, also negatively regulates atrophy by preventing the binding of FoxO to atrophy-related genes (Bonaldo and Sandri, 2013; Qin et al., 2010; Sandri et al., 2006). Therefore, the increase in both isoforms likely contributed to the hypertrophy and increased muscle mass observed with formoterol treatment. By 21 DPI no differences in PGC-1α expression or that of either isoform was detected, suggesting that, similar to that reported previously in the spinal cord (Scholpa et al., 2019), early formoterol-induced increases in skeletal muscle PGC-1α expression contribute to the improved recovery observed at later time points.

While skeletal muscle has a large capacity for regeneration, there are insufficient pharmacological interventions for muscle atrophy (Perez-Schindler et al., 2013). As such, exercise training is one of the more common methods to not only combat muscle loss, but to also assess molecular regulation of muscle remodeling (Perez-Schindler et al., 2013). In support of pharmacologically targeting MB to treat atrophy, exercise has been shown to increase mitochondrial mass and function, even in paralyzed muscle (O'Brien and Gorgey, 2016; Sato et al., 2011). Concurrently, active muscle contractions have been shown to induce PGC-1α in the skeletal muscle of both rodents and humans, with increases being observed after as little as one bout of exercise (Baar et al., 2002; Petrie et al., 2016; Pilegaard et al., 2003). Furthermore, transgenic overexpression of PGC-1α in muscle protects against muscle atrophy (Dinulovic et al., 2016), and promotes MB and oxidative metabolism[36], while muscle-specific PGC-1α knockout mice exhibit reduced oxidative muscle fibers and decreased exercise endurance (Handschin et al., 2007). These published data provide evidence for both the importance of PGC-1α in skeletal muscle health, and the potential for pharmacological induction of PGC-1α following various forms of muscle loss, including post-SCI.

Approximately 90% of all β-adrenergic receptors in the skeletal muscle are the ADRB2 subtype (Jensen et al., 1995), indicative of their importance within this tissue. ADRB2 KO mice exhibited altered basal expression of mitochondrial function-related proteins, including PGC-1α, suggesting that this receptor may play a physiological role in skeletal muscle mitochondrial homeostasis and atrophy/hypertrophy. In support of this idea, exercise-induced PGC-1α is largely attenuated by pretreatment with the ADRB2-specific inhibitor, ICI-118,551, in uninjured mice, indicating that this induction and any subsequent MB is partially mediated by ADRB2 activation (Miura et al., 2007). Furthermore, exercise improves oxidative performance in part through increasing muscle ADRB2 density (Sato et al., 2011). Importantly, formoterol had no effect in ADRB2 KO mice post-SCI, indicating that formoterol-induced recovery occurs through agonism of this receptor.

Because of the role of exercise in combating skeletal muscle atrophy, it is difficult to distinguish the beneficial effects of formoterol-induced MB from those of the increased locomotor capability in these mice. Formoterol treatment improves functional recovery, leading to increased movement of the hindlimbs, which is likely contributing to the decrease in skeletal muscle atrophy. Unlike markers of MB, differences in markers of atrophy and hypertrophy were more pronounced in formoterol-treated injured mice 21 DPI compared to 3 DPI. This could suggest that these effects are dependent, at least in part, on the eventual increase in motor activity in formoterol-treated injured mice.

Given the aforementioned published data in addition to that presented here, it would be interesting to assess the effect of formoterol treatment in conjunction with an exercise training regimen post-SCI. It is important to note, however, that excessive activation of ADRB2, whether it be pharmacologically or through exercise, can induce downregulation and desensitization of the receptor (Sato et al., 2011). Therefore, care must be taken to ensure that any intervention is not so vigorous as to negate the beneficial effects. Nonetheless, the data reported here provide evidence for the use of systemic ADRB2 agonism with the FDA-approved compound formoterol for the comprehensive treatment of SCI, addressing both spinal cord and skeletal muscle complications.

Author disclosure statement

No competing financial interests exist.

Funding

This work was supported by the Department of Defense Spinal Cord Injury Research Program [SC180122]; National Institutes of Health National Institute of General Medical Sciences [GM084147]; and the Biomedical Laboratory Research and Development Program of the Department of Veterans Affairs [BX: 000851]. The imaging core is funded by the National Institutes of Health [S10 OD011981].

Acknowledgements

We would like to thank the University of Arizona, Imaging Cores – Life Sciences North and Dr. William A. Day for assistance with EM processing and imaging.

References

Baar, K., Wende, A.R., Jones, T.E., Marison, M., Nolte, L.A., Chen, M., Kelly, D.P., Holloszy, J.O., 2002. Adaptations of skeletal muscle to exercise: rapid increase in the transcriptional coactivator PGC-1. FASEB J. 16, 1879–1886.

Basso, D.M., Fisher, L.C., Anderson, A.J., Jakeman, L.B., McTigue, D.M., Popovich, P.G., 2006. Basso mouse scale for locomotion detects differences in recovery after spinal cord injury in five common mouse strains. J. Neurotrauma 23, 635–659.
Beitzel, F., Gregorevic, P., Ryall, J.G., Plant, D.R., Sillence, M.N., Lynch, G.S., 2004. Beta2-adrenoceptor agonist fenoterol enhances functional repair of regenerating rat skeletal muscle after injury. J. Appl. Physiol. 96, 1385–1392 (Bethesda, Md. : 1985).
Bodine, S.C., Stitt, T.N., Gonzalez, M., Kline, W.O., Stover, G.L., Bauerlein, R., Zlotchenko, E., Scrimgeour, A., Lawrence, J.C., Glass, D.J., Yancopoulos, G.D., 2001. Akt/mTOR pathway is a crucial regulator of skeletal muscle hypertrophy and can prevent muscle atrophy in vivo. Nat. Cell Biol. 3, 1014–1019.
Bonaldo, P., Sandri, M., 2013. Cellular and molecular mechanisms of muscle atrophy. Dis. Model. Mech. 6, 25–39.
Brunet, A., Bonni, A., Zigmond, M.J., Lin, M.Z., Juo, P., Hu, L.S., Anderson, M.J., Arden, K.C., Blenis, J., Greenberg, M.E., 1999. Akt promotes cell survival by phosphorylating and inhibiting a Forkhead transcription factor. Cell 96, 857–868.
Castro, M.J., Apple Jr., D.F., Hillegass, E.A., Dudley, G.A., 1999. Influence of complete spinal cord injury on skeletal muscle cross-sectional area within the first 6 months of injury. Eur. J. Appl. Physiol. Occup. Physiol. 80, 373–378.
De Gasperi, R., Graham, Z.A., Harlow, L.M., Bauman, W.A., Qin, W., Cardozo, C.P., 2016. The signature of MicroRNA dysregulation in muscle paralyzed by spinal cord injury includes downregulation of MicroRNAs that target myostatin signaling. PLoS One 11, e0166189.
Dinulovic, I., Furrer, R., Di Fulvio, S., Ferry, A., Beer, M., Handschin, C., 2016. PGC-1α modulates necrosis, inflammatory response, and fibrotic tissue formation in injured skeletal muscle. Skelet. Muscle 6, 38.
Gorgey, A.S., Dolbow, D.R., Dolbow, J.D., Khalil, R.K., Castillo, C., Gater, D.R., 2014. Effects of spinal cord injury on body composition and metabolic profile - part I. J. Spinal Cord Med. 37, 693–702.
Gorgey, A.S., Witt, O., O'Brien, L., Cardozo, C., Chen, Q., Lesnefsky, E.J., Graham, Z.A., 2019. Mitochondrial health and muscle plasticity after spinal cord injury. Eur. J. Appl. Physiol. 119, 315–331.
Graham, Z.A., Collier, L., Peng, Y., Saez, J.C., Bauman, W.A., Qin, W., Cardozo, C.P., 2016. A soluble activin receptor IIB fails to prevent muscle atrophy in a mouse model of spinal cord injury. J. Neurotrauma 33, 1128–1135.
Grisanti, L.A., Thomas, T.P., Carter, R.L., de Lucia, C., Gao, E., Koch, W.J., Benovic, J.L., Tilley, D.G., 2018. Pepducin-mediated cardioprotection via β-arrestin-biased β2-adrenergic receptor-specific signaling. Theranostics 8, 4664–4678.
Handschin, C., Chin, S., Li, P., Liu, F., Maratos-Flier, E., Lebrasseur, N.K., Yan, Z., Spiegelman, B.M., 2007. Skeletal muscle fiber-type switching, exercise intolerance, and myopathy in PGC-1alpha muscle-specific knock-out animals. J. Biol. Chem. 282, 30014–30021.
Harcourt, L.J., Schertzer, J.D., Ryall, J.G., Lynch, G.S., 2007. Low dose formoterol administration improves muscle function in dystrophic mdx mice without increasing fatigue. Neuromuscul. Disord.: NMD 17, 47–55.
Hojlund, K., Mogensen, M., Sahlin, K., Beck-Nielsen, H., 2008. Mitochondrial dysfunction in type 2 diabetes and obesity. Endocrinol. Metab. Clin. N. Am. 37, 713–731 (x).
Jensen, J., Brors, O., Dahl, H.A., 1995. Different beta-adrenergic receptor density in different rat skeletal muscle fibre types. Pharmacol. Toxicol. 76, 380–385.
Jesinkey, S.R., Funk, J.A., Stallons, L.J., Wills, L.P., Megyesi, J.K., Beeson, C.C., Schnellmann, R.G., 2014a. Formoterol restores mitochondrial and renal function after ischemia-reperfusion injury. J. Am. Soc. Nephrol. 25, 1157–1162.
Jesinkey, S.R., Korrapati, M.C., Rasbach, K.A., Beeson, C.C., Schnellmann, R.G., 2014b. Atomoxetine prevents dexamethasone-induced skeletal muscle atrophy in mice. J. Pharmacol. Exp. Ther. 351, 663–673.
Jesinkey, S.R., Korrapati, M.C., Rasbach, K.A., Beeson, C.C., Schnellmann, R.G., 2014c. Atomoxetine prevents dexamethasone-induced skeletal muscle atrophy in mice. J. Pharmacol. Exp. Ther. 351, 663–673.
Joassard, O.R., Amirouche, A., Gallot, Y.S., Desgeorges, M.M., Castells, J., Durieux, A.C., Berthon, P., Freyssenet, D.G., 2013. Regulation of Akt-mTOR, ubiquitin-proteasome and autophagy-lysosome pathways in response to formoterol administration in rat skeletal muscle. Int. J. Biochem. Cell Biol. 45, 2444–2455.
Kelley, D.E., He, J., Menshikova, E.V., Ritov, V.B., 2002. Dysfunction of mitochondria in human skeletal muscle in type 2 diabetes. Diabetes 51, 2944–2950.
Landry, E., Frenette, J., Guertin, P.A., 2004. Body weight, limb size, and muscular properties of early paraplegic mice. J. Neurotrauma 21, 1008–1016.
Lecker, S.H., Jagoe, R.T., Gilbert, A., Gomes, M., Baracos, V., Bailey, J., Price, S.R., Mitch, W.E., Goldberg, A.L., 2004. Multiple types of skeletal muscle atrophy involve a common program of changes in gene expression. FASEB J. 18, 39–51.
Martin, T.P., Stein, R.B., Hoeppner, P.H., Reid, D.C., 1992. Influence of electrical stimulation on the morphological and metabolic properties of paralyzed muscle. J. Appl. Physiol. (Bethesda, Md. : 1985) 72, 1401–1406.
Martinez-Redondo, V., Jannig, P.R., Correia, J.C., Ferreira, D.M., Cervenka, I., Lindvall, J.M., Sinha, I., Izadi, M., Pettersson-Klein, A.T., Agudelo, L.Z., Gimenez-Cassina, A., Brum, P.C., Dahlman-Wright, K., Ruas, J.L., 2016. Peroxisome proliferator-activated receptor gamma coactivator-1 alpha isoforms selectively regulate multiple splicing events on target genes. J. Biol. Chem. 291, 15169–15184.
McCully, K.K., Mulcahy, T.K., Ryan, T.E., Zhao, Q., 2011. Skeletal muscle metabolism in individuals with spinal cord injury. J. Appl. Physiol. 111, 143–148 (Bethesda, Md. : 1985).
Miura, S., Kawanaka, K., Kai, Y., Tamura, M., Goto, M., Shiuchi, T., Minokoshi, Y., Ezaki, O., 2007. An increase in murine skeletal muscle peroxisome proliferator-activated receptor-gamma coactivator-1alpha (PGC-1alpha) mRNA in response to exercise is mediated by beta-adrenergic receptor activation. Endocrinology 148, 3441–3448.
Monroe, M.B., Tataranni, P.A., Pratley, R., Manore, M.M., Skinner, J.S., Ravussin, E., 1998. Lower daily energy expenditure as measured by a respiratory chamber in subjects with spinal cord injury compared with control subjects. Am. J. Clin. Nutr. 68, 1223–1227.
Montgomery, M.K., Turner, N., 2015. Mitochondrial dysfunction and insulin resistance: an update. Endocr. Connect. 4, R1–R15.
National Spinal Cord Injury Statistical Center, 2019. Facts and Figures at a Glance. University of Alabama at Birmingham, Birmingham, AL.
O'Brien, L.C., Gorgey, A.S., 2016. Skeletal muscle mitochondrial health and spinal cord injury. World J. Orthop. 7, 628–637.
Patel, S.P., Cox, D.H., Gollihue, J.L., Bailey, W.M., Geldenhuys, W.J., Gensel, J.C., Sullivan, P.G., Rabchevsky, A.G., 2017. Pioglitazone treatment following spinal cord injury maintains acute mitochondrial integrity and increases chronic tissue sparing and functional recovery. Exp. Neurol. 293, 74–82.
Perez-Schindler, J., Summermatter, S., Santos, G., Zorzato, F., Handschin, C., 2013. The transcriptional coactivator PGC-1alpha is dispensable for chronic overload-induced skeletal muscle hypertrophy and metabolic remodeling. Proc. Natl. Acad. Sci. U. S. A. 110, 20314–20319.
Petrie, M.A., Kimball, A.L., McHenry, C.L., Suneja, M., Yen, C.L., Sharma, A., Shields, R.K., 2016. Distinct skeletal muscle gene regulation from active contraction, passive vibration, and whole body heat stress in humans. PLoS One 11, e0160594.
Pilegaard, H., Saltin, B., Neufer, P.D., 2003. Exercise induces transient transcriptional activation of the PGC-1alpha gene in human skeletal muscle. J. Physiol. 546, 851–858.
Powell, D., Affuso, O., Chen, Y., 2017. Weight change after spinal cord injury. J. Spinal Cord Med. 40, 130–137.
Qin, W., Pan, J., Wu, Y., Bauman, W.A., Cardozo, C., 2010. Protection against dexamethasone-induced muscle atrophy is related to modulation by testosterone of FOXO1 and PGC-1alpha. Biochem. Biophys. Res. Commun. 403, 473–478.
Ruas, J.L., White, J.P., Rao, R.R., Kleiner, S., Brannan, K.T., Harrison, B.C., Greene, N.P., Wu, J., Estall, J.L., Irving, B.A., Lanza, I.R., Rasbach, K.A., Okutsu, M., Nair, K.S., Yan, Z., Leinwand, L.A., Spiegelman, B.M., 2012. A PGC-1alpha isoform induced by resistance training regulates skeletal muscle hypertrophy. Cell 151, 1319–1331.
Sandri, M., Sandri, C., Gilbert, A., Skurk, C., Calabria, E., Picard, A., Walsh, K., Schiaffino, S., Lecker, S.H., Goldberg, A.L., 2004. Foxo transcription factors induce the atrophy-related ubiquitin ligase atrogin-1 and cause skeletal muscle atrophy. Cell 117, 399–412.
Sandri, M., Lin, J., Handschin, C., Yang, W., Arany, Z.P., Lecker, S.H., Goldberg, A.L., Spiegelman, B.M., 2006. PGC-1alpha protects skeletal muscle from atrophy by suppressing FoxO3 action and atrophy-specific gene transcription. Proc. Natl. Acad. Sci. U. S. A. 103, 16260–16265.
Sato, S., Shirato, K., Tachiyashiki, K., Imaizumi, K., 2011. Muscle plasticity and beta(2)-adrenergic receptors: adaptive responses of beta(2)-adrenergic receptor expression to muscle hypertrophy and atrophy. J. Biomed. Biotechnol. 2011, 729598.
Scelsi, R., Marchetti, C., Poggi, P., Lotta, S., Lommi, G., 1982. Muscle fiber type morphology and distribution in paraplegic patients with traumatic cord lesion. Histochemical and ultrastructural aspects of rectus femoris muscle. Acta Neuropathol. 57, 243–248.
Scholpa, N.E., Schnellmann, R.G., 2017. Mitochondrial-based therapeutics for the treatment of spinal cord injury: mitochondrial biogenesis as a potential pharmacological target. J. Pharmacol. Exp. Ther. 363, 303–313.
Scholpa, N.E., Williams, H., Wang, W., Corum, D., Narang, A., Tomlinson, S., Sullivan, P.G., Rabchevsky, A.G., Schnellmann, R.G., 2019. Pharmacological stimulation of mitochondrial biogenesis using the food and drug administration-approved beta2-adrenoreceptor agonist formoterol for the treatment of spinal cord injury. J. Neurotrauma 36, 962–972.
Toledo, F.G., Goodpaster, B.H., 2013. The role of weight loss and exercise in correcting skeletal muscle mitochondrial abnormalities in obesity, diabetes and aging. Mol. Cell. Endocrinol. 379, 30–34.
Urso, M.L., Chen, Y.W., Scrimgeour, A.G., Lee, P.C., Lee, K.F., Clarkson, P.M., 2007. Alterations in mRNA expression and protein products following spinal cord injury in humans. J. Physiol. 579, 877–892.
Wills, L.P., Trager, R.E., Beeson, G.C., Lindsey, C.C., Peterson, Y.K., Beeson, C.C., Schnellmann, R.G., 2012. The beta2-adrenoceptor agonist formoterol stimulates mitochondrial biogenesis. J. Pharmacol. Exp. Ther. 342, 106–118.
Zeman, R.J., Ludemann, R., Etlinger, J.D., 1987. Clenbuterol, a beta 2-agonist, retards atrophy in denervated muscles. Am. J. Phys. 252, E152–E155.